Density Functional Theory and Electron Paramagnetic Resonance Study on the Effect of N−F Codoping of TiO_2

C. Di Valentin,* E. Finazzi, and G. Pacchioni

Dipartimento di Scienza dei Materiali, Università di Milano-Bicocca, Via R. Cozzi, 53, 20125 Milano, Italy

A. Selloni

Department of Chemistry, Princeton University, Princeton, New Jersey 08540

S. Livraghi, A. M. Czoska, M. C. Paganini, and E. Giamello

Dipartimento di Chimica IFM, Università di Torino and NIS, Nanostructured Interfaces and Surfaces Centre of Excellence, Via P. Giuria 7, I - 10125 Torino, Italy

Received December 20, 2007. Revised Manuscript Received February 29, 2008

Recent experiments have indicated that titanium dioxide (TiO_2) codoped with nitrogen and fluorine may show enhanced photocatalytic activity in the visible region with respect to TiO_2 doped only with nitrogen. Prompted by these findings, we have investigated N−F codoped TiO_2 through a combined theoretical and experimental study. Density functional theory (DFT) calculations have been carried out both within the generalized gradient approximation (GGA) and using hybrid functionals to accurately describe the electronic structure; substitutional as well as interstitial locations of nitrogen in the TiO_2 lattice were considered. From these calculations we infer that N−F codoping reduces the energy cost of doping and also the amount of defects (number of oxygen vacancies) in the lattice, as a consequence of the charge compensation between the nitrogen (p-dopant) and the fluorine (n-dopant) impurities. The UV−visible spectra of the sol−gel prepared TiO_2 powders confirm the synergistic effect of N−F codoping: more impurities are introduced in the lattice with an increased optical absorption in the visible. EPR spectroscopy measurements on the codoped samples identify two paramagnetic species which are associated to bulk N impurities ($N_b^{\bullet}$) and Ti^{3+} ions. Preliminary photocatalytic tests also indicate an enhanced activity under vis-light irradiation toward degradation of methylene blue for the codoped system with respect to N-doped TiO_2.

1. Introduction

Doping is a promising approach to reduce the absorption threshold of titanium dioxide (TiO_2) and bring it from the UV to the visible region.[1] For this reason a large number of investigations have focused on doping of TiO_2 with both metal and nonmetal elements over the past decade.[2–4] Still, the photocatalytic performance of doped TiO_2 in the visible is usually found to be less satisfactory than that of pure TiO_2 under UV irradiation.[5,6] In fact, the absorption in the visible, although improved by doping, remains scarce, while the recombination rate of the charge carriers increases in the doped samples,[7] because dopants may themselves be recombination centers or generate other defects such as oxygen vacancies. A possible way to improve the photocatalytic performance of doped TiO_2 is to exploit the cooperative effect of introducing different dopants into the matrix. As shown in a recent communication,[8] however, codoping is not a guarantee of success, indicating that a careful analysis and evaluation of the choice of codopants is important.

Recent experimental studies have reported a remarkable photocatalytic activity of nitrogen and fluorine codoped TiO_2 under visible light.[9,10] With the goal to clarify the physical origin of these observations, in this paper we report on a combined theoretical and experimental study of N−F codoped anatase TiO_2 (N−F/TiO_2). Theoretical investigations provide detailed microscopic information on the electronic structure of the system and are therefore useful to identify a "good pair" of dopants with potential synergistic effects.

A useful prerequisite for understanding cooperative effects in codoping is the precise knowledge of the two separately

* Corresponding author. E-mail: cristiana.divalentin@mater.unimib.it.

(1) Asahi, R.; Morikawa, T.; Ohwaki, T.; Aoki, K.; Taga, Y. *Science* **2001**, *293*, 269.
(2) Thompson, T. L.; Yates, J. T., Jr. *Chem. Rev.* **2006**, *106*, 4428.
(3) Chen, X.; Mao, S. S. *Chem. Rev.* **2007**, *107*, 2891.
(4) Special Issue in Chemical Physics: Doping and functionalization of photo-active semiconducting oxides. *Chem. Phys.* **2007**, *339*, 1−192 (Guest Editors: Di Valentin, C., Diebold, C., Selloni, A.).
(5) Mrowetz, M.; Balcerski, W.; Colussi, A. J.; Hoffmann, M. R. *J. Phys Chem. B* **2004**, *108*, 17269.
(6) Tachikawa, T.; Takai, Y.; Tojo, S.; Fujitsuka, M.; Irie, H.; Hashimoto, K.; Majima, T. *J. Phys. Chem. B* **2006**, *110*, 13158.
(7) Beranek, R.; Neumann, B.; Sakthivel, S.; Janczarek, M.; Dittrich, T.; Tributsch, H.; Kisch, H. *Chem. Phys.* **2007**, *339*, 11.
(8) In, S.; Orlov, A.; Berg, R.; Garcia, F.; Pedrosa-Jimenez, S.; Tikhov, M. S.; Wright, D. S.; Lambert, R. M. *J. Am. Chem. Soc.* **2007**, *129*, 13790.
(9) (a) Li, D.; Haneda, H.; Hishita, S.; Ohashi, N. *Chem. Mater.* **2005**, *17*, 2588. (b) Li, D.; Haneda, H.; Hishita, S.; Ohashi, N. *Chem. Mater.* **2005**, *17*, 2596. (c) Li, D.; Ohashi, N.; Hishita, S.; Kolodiazhnyi, T.; Haneda, H. *J. Solid State Chem.* **2005**, *178*, 3293.
(10) Huang, D.-G.; Liao, S.-J.; Liu, J.-M.; Dang, Z.; Petrik, L. *J. Photochem. Photobiol., A: Chem.* **2006**, *184*, 282.

10.1021/cm703636s CCC: $40.75
Published on Web 05/07/2008

Scheme 1

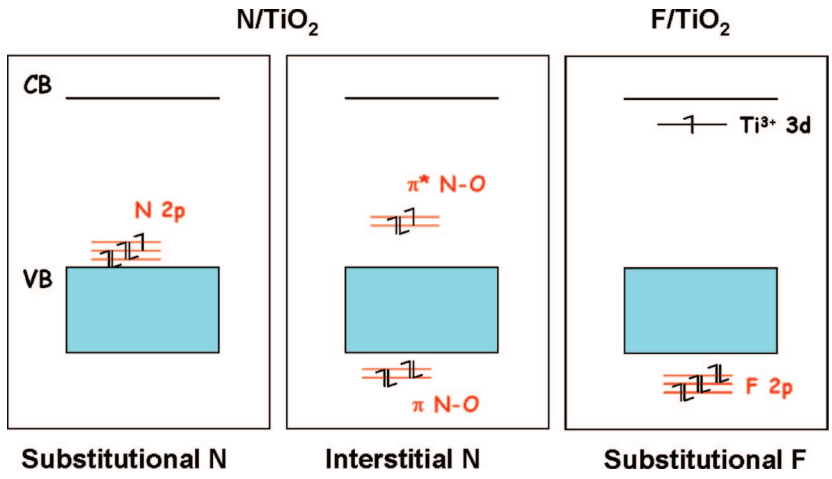

doped systems. For N-doped TiO_2 (N/TiO_2), several studies have been reported,[1–3] including a series of papers from our group.[11] The electronic structure of nitrogen substitutional and interstitial impurities has been clarified,[11a,b] as well as the stabilizing interaction between impurities and oxygen vacancies in reduced TiO_2.[11b,d] The N-impurities give rise to localized states just above the valence band (few tenths of an electronvolt) and also cause a drastic reduction of the cost of formation of oxygen vacancies as a consequence of electron transfer from the O-vacancies derived Ti^{3+} states to the partially unoccupied nitrogen states.[11d] As to the doping with fluorine, in a recent combined density functional theory (DFT) and electron paramagnetic resonance (EPR) study of F-doped TiO_2 (F/TiO_2) we have found that (substitutional) F-dopants induce the formation of Ti^{3+} species in the bulk of anatase polycrystalline TiO_2 samples, with consequent formation of Ti 3d occupied states in the band gap, some tenths of an electronvolt below the conduction band.[12] A simple sketch of the electronic structure of the N-doped (both substitutional to O and interstitial) and F-doped systems is given in Scheme 1. In the following we will present new results for the N−F codoped system obtained by means of DFT calculations and a number of experimental techniques. The doped samples were synthesized through the sol−gel technique and characterized by X-ray diffraction (XDR), UV−visible, and EPR spectroscopy. Some preliminary comparative photocatalytic tests were also performed for the photodegradation of methylene blue under visible light irradiation.

2. Computational Details

The calculations were performed including spin polarization and using both the generalized gradient approximation (GGA) with the PBE[13] functional and the hybrid B3LYP[14] functional. The percentage of exact Hartree−Fock (HF) exchange in the B3LYP functional is 20%. For the GGA-PBE calculations a plane wave basis set was used. The cutoffs for the smooth part of the wave function and the augmented density were 25 and 200 Ry, respectively, as implemented in the Quantum ESPRESSO code.[15] For the hybrid functional calculations the Kohn−Sham orbitals are expanded in Gaussian type Orbitals (GTO), as implemented in the CRYSTAL06 code[16](the all-electron basis-sets are Ti 86411(d41) [ref 17], O 8411(d1) [ref 18], N 7311(d1) [ref 19], and F 7311 [ref 20]). For an improved description of the Ti^{3+} species we have added a more diffuse d function with α exponent = 0.13.

We considered a nearly cubic $2\sqrt{2} \times 2\sqrt{2} \times 1$ supercell to model doped anatase. The optimized bulk lattice parameters were taken from previous PBE (a = 3.786 Å, and c = 9.737 Å)[21] and B3LYP (a = 3.776 Å, and c = 9.866 Å)[22] calculations. N_s-F_s codoping (s = substitutional) was modeled by replacing two oxygen atoms in the 96-atoms supercell. The resulting stoichiometry is $TiO_{2-2x}N_xF_x$ with x = 0.031. N_i-F_s codoping (i = interstitial) was modeled by adding one N atom to the system and replacing one O atom with one F atom in the 96-atom supercell. The resulting stoichiometry in this case is $TiO_{2-x}N_xF_x$ with x = 0.031. N_b (b = bulk) will also be used in the following as a general reference to both N_s and N_i present in the bulk of TiO_2.

Full geometry optimization was performed until the largest component of the ionic forces was less than 5×10^{-4} au.

(11) (a) Di Valentin, C.; Pacchioni, G.; Selloni, A. *Phys. Rev. B* **2004**, *700*, 85116. (b) Di Valentin, C.; Pacchioni, G.; Selloni, A.; Livraghi, S.; Giamello, E. *J. Phys Chem. B* **2005**, *109*, 11414–11419. (c) Livraghi, S.; Votta, A; Paganini, M. C.; Giamello, E. *Chem. Commun.* **2005**, 498–500. (d) Livraghi, S.; Paganini, M. C.; Giamello, E.; Selloni, A; Di Valentin, C.; Pacchioni, G. *J. Am. Chem. Soc.* **2006**, *128*, 15666. (e) Di Valentin, C.; Finazzi, E.; Pacchioni, G.; Selloni, A.; Livraghi, S.; Paganini, M. C.; Giamello, E. *Chem. Phys.* **2007**, *339*, 44. (f) Finazzi, E.; Di Valentin, C.; Selloni, A.; Pacchioni, G. *J. Phys. Chem. C* **2007**, *111*, 9275.
(12) Czoska, A. M. ; Livraghi, S.; Chiesa, M.; Giamello, E.; Finazzi, E.; Di Valentin, C.; Pacchioni, G. *J. Phys. Chem. C* **2008**, in press.
(13) Perdew, P.; Burke, K.; Ernzerhof, M. *Phys. Rev. Lett.* **1996**, *77*, 3865.
(14) (a) Becke, A. D. *J. Chem. Phys.* **1993**, *98*, 5648. (b) Lee, C.; Yang, W.; Parr, R. G. *Phys. Rev. B* **1988**, *37*, 785.
(15) Baroni, S.; et al. http://www.pwscf.org (accessed July 2007).
(16) Saunders, V. R.; Dovesi, R.; Roetti, C.; Orlando, R.; Zicovich-Wilson, C. M.; Harrison, N. M.; Doll, K.; Civalleri, B.; Bush, I. J.; D'Arco, Ph.; Llunell, M. *CRYSTAL03 User's Manual*; University of Torino: Torino: 2003.
(17) Zicovich-Wilson, C. M.; Dovesi, R. *J. Phys. Chem. B* **1998**, *102*, 1411.
(18) Ruiz, E.; Llunlell, M.; Alemany, P. *J. Solid State Chem.* **2003**, *176*, 400.
(19) Padey, R.; Jaffe, J. E.; Harrison, N. M. *J. Phys. Chem. Solids* **1994**, *55*, 1357.
(20) Nada, R.; Catlow, C. R. A.; Pisani, C.; Orlando, R. *Modell. Simul. Mater. Sci. Eng.* **1993**, *1*, 165.
(21) Lazzeri, M.; Vittadini, A.; Selloni, A. *Phys. Rev. B* **2001**, *63*, 155409.
(22) Zhang, Y.; Lin, W.; Ding, K.; Li, J. *J. Phys. Chem. B* **2005**, *109*, 19270.

The *k*-space sampling was restricted to a special *k*-point, in the irreducible part of the Brillouin zone,[11] for the plane wave self-consistent field (PWSCF) calculations, and to the Γ-point for the CRYSTAL calculations. The CRYSTAL densities of states (DOS) have been obtained with a 36 *k*-point mesh.

3. Experimental Details

Bare TiO_2 was prepared via sol−gel, mixing a solution of titanium(IV) isopropoxide in isopropylic alcohol with water. N/TiO_2 and $N-F/TiO_2$ samples were prepared in the same way as TiO_2 using, instead of water, a solution of NH_4Cl and NH_4F, respectively. While N and F are introduced in the lattice in substitutional position to O, Cl is not because of its too large atomic size. The gel was left aging for 15 h at room temperature and subsequently dried at 70 °C. The dried material was eventually calcined in air at 770 K for 1 h. In the case of N,F-codoped TiO_2 the nominal N/F ratio is 1. The actual N/F ratio in the prepared materials is probably different from the nominal one which is referenced to the solution composition. Samples with increasing N/F ratio (nominal ratios of 10 and 100, respectively) were prepared dosing ammonium chloride and ammonium fluoride in the solution maintaining constant the NH_4^+ concentration in all cases. In the following we will refer, for the various samples, to the N/F ratio of the solutions being aware that the actual concentration in the solid is not in principle the same.

The structures of the prepared materials were determined by X-ray diffraction (XRD) using a Philips 1830 diffractometer with a Co Kα source. A X'Peret High-Score software was adopted for data handling. Diffuse reflectance UV−visible (DR UV−vis) spectra were recorded by a Varian Cary 5 spectrometer using a Cary win-UV/scan software. Electron paramagnetic resonance (EPR) spectra were run on a X-band CW Bruker EMX spectrometer equipped with a cylindrical cavity and operating at a 100 KHz field modulation. Computer simulation of the spectra were obtained using the SIM32 program.[23] A catalytic test on the photodegradation of methylene blue with monochromatic visible light ($\lambda = 437$ nm) was performed following the procedure reported by Burda et al.[24]

4. Results and Discussion

4.1. Theoretical Calculations. *4.1.1. N_s-F_s Codoping.* We have chosen the positions of the N and F impurity atoms in the 96-atoms anatase bulk supercell so that their distance is about 6 Å.[25] Both N and F impurities have an odd number of valence electrons. When introduced at O substitutional sites in the TiO_2 bulk matrix, two possible configurations can occur: either the two unpaired electrons remain unpaired, possibly localized on two different sites (triplet configuration), or they pair up either on one of the two dopant sites or somewhere else (singlet configuration). Both electronic configurations have been considered in the present study. The densities of states (DOS) for the triplet and singlet configurations obtained using the GGA-PBE (with the plane-wave pseudopotential scheme) are reported in Figure 1a,b, where the projected densities of states (PDOS) on the impurity atoms are also shown.

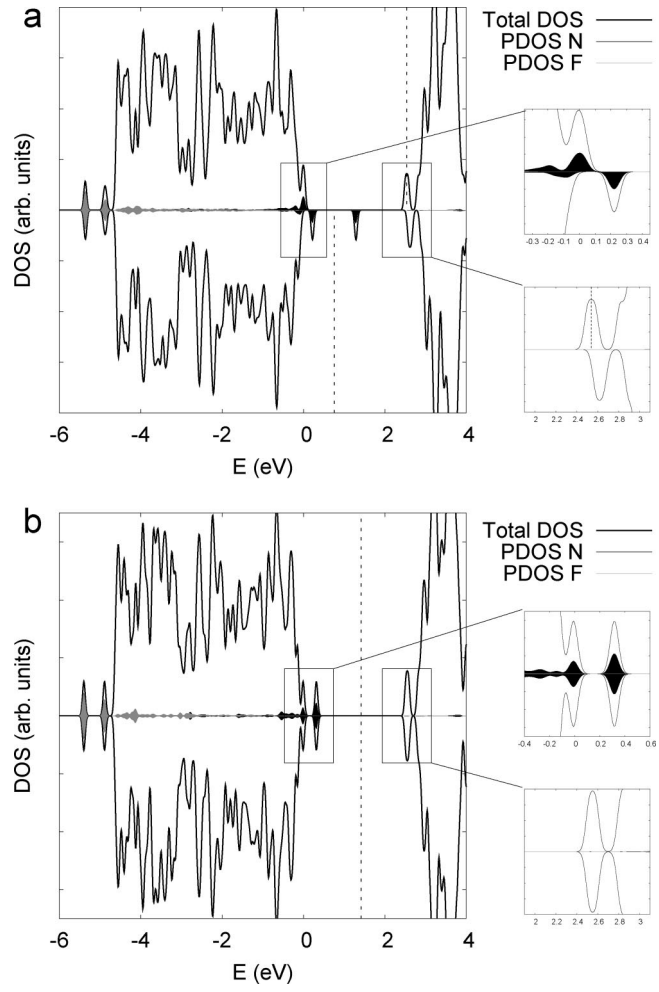

Figure 1. Total and projected (black, on N atom; grey, on F atom) density of states from the PBE calculation for the (a) triplet and (b) singlet N_s-F_s/TiO_2. The zero energy value is set at the top of the valence band. States below and above the dotted vertical line are occupied and unoccupied, respectively.

We start considering the DOS for the triplet configuration which is found to be essentially the result of the superposition of the separate DOS for the N/TiO_2 and F/TiO_2 systems,[11a,12] without any significant modification resulting from the interaction between the two dopants. The impurity states fall in very different energy regions: the F 2p states fall well below the bottom of the O 2p valence band, while the N 2p states fall just above the top of the O 2p valence band. The Fermi energy lies high up in the band gap, and crosses a narrow Ti 3d band, almost at the conduction band edge. The same electronic structure feature is found for the F-doped system because the F-dopant behaves as an n-donor and introduces an extra electron in the system.[12] In GGA the high energy state in the gap (at the CB edge) is largely delocalized on several Ti atoms, consistent with the fact that the corresponding state is nearly in the conduction band. The other electron of the triplet state is fully localized on the N atom ($N_s^{\bullet}$, see the spin density plot reported in the Supporting Information, Figure S1). The spin delocalization of the Ti 3d states is known to be an artifact of local (LDA) and

(23) Adamski, A.; Spalek, T.; Sojka, Z. *Res. Chem. Intermed.* **2003**, *29*, 793.
(24) Burda, C.; Lou, Y.; Chen, X.; Samia, A. C.; Stout, S.; Gole, J. J. L. *Nano Lett.* **2003**, *3*, 1049.
(25) The possibility that the two dopants may cluster was considered by performing a PBE calculation with a nitrogen and a fluorine atom separated by only one titanium atom. This configuration is only slightly more stable (0.15 eV) than the one considered in the manuscript. The analysis of the electronic structure reported in the text is correct for both configurations which differ only for nonrelevant details.

Scheme 2

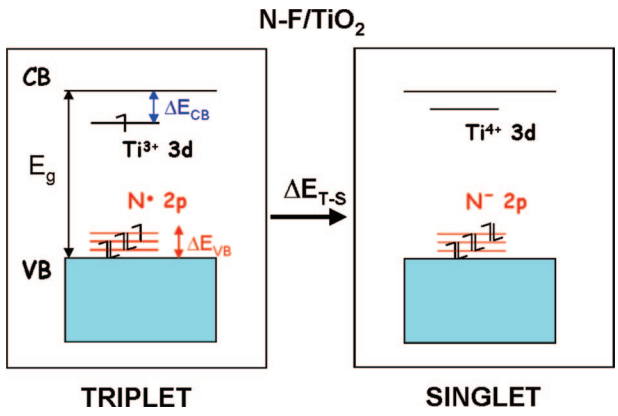

semilocal (GGA) DFT functionals, found also for other paramagnetic defects in wide-gap semiconductors and insulators.[26,27] This is caused by the fact that these functionals do not fully remove the electron self-interaction and therefore tend to overestimate electron delocalization. We have previously shown for the case of the O-vacancy on the rutile (110) surface[28] that this difficulty can be largely overcome by the use of a hybrid functional such as B3LYP, which includes some exact HF exchange and thus corrects for the on-site Coulomb repulsion. A description of N−F/TiO_2, based on the B3LYP hybrid functional, will be presented in the following.

If the electron in the Ti 3d state pairs up with the unpaired electron in the N 2p states (starting triplet configuration: $N_s^{\bullet}$ + Ti^{3+}) the overall spin configuration of the system becomes a closed shell singlet (final singlet configuration: N_s^{-} + Ti^{4+}). In this case (Figure 1b), the Fermi energy of the system corresponds to the highest N 2p state, a few tenths of an eV above the valence band. This pairing has a strong stabilizing effect which can be estimated as the difference in the total energy between the two spin configurations. It amounts to 1.75 eV and corresponds to $\Delta E_{T\text{-}S}$ in Scheme 2. In the experimental section 4.2 we will show that the electron transfer just proposed is supported by the experimental findings. A similar stabilizing effect, a case of negative Hubbard U, was already predicted by us, and confirmed in later studies,[29] for electrons in Ti^{3+} states associated to oxygen vacancies in reduced TiO_2 systems.[11b,d] In this case the extent of stabilization is such that N-doped samples probably include a large number of oxygen vacancies, as indicated by some experimental works.[30–32] In the present context of N−F/TiO_2, the Ti^{3+} species are formed in association to the substitutional F-doping. No oxygen vacancies are required to induce extra electrons available to fill the N 2p states with the relevant consequence that a smaller number of oxygen defects should be present in the bulk of the N−F codoped TiO_2 samples than in an N-doped counterpart. This could be the reason of the larger photostability and photocatalytic activity of the codoped sample studied in ref 9. In fact, it is generally assumed that oxygen vacancies act as efficient recombination centers, drastically reducing the charge carrier lifetimes.[33,34] If the number of O vacancies is smaller, then the photocatalytic efficiency is expected be improved, as reported for O_2 evolution from aqueous silver nitrate solution under vis-light irradiation of Cr−Sb codoped TiO_2.[35]

As shown previously,[28] hybrid functionals provide a satisfactory description of the localized nature of the $3d^1$ Ti^{3+} state associated with the presence of O vacancies, OH groups, or F-dopants,[12] and also improve the evaluation of the band

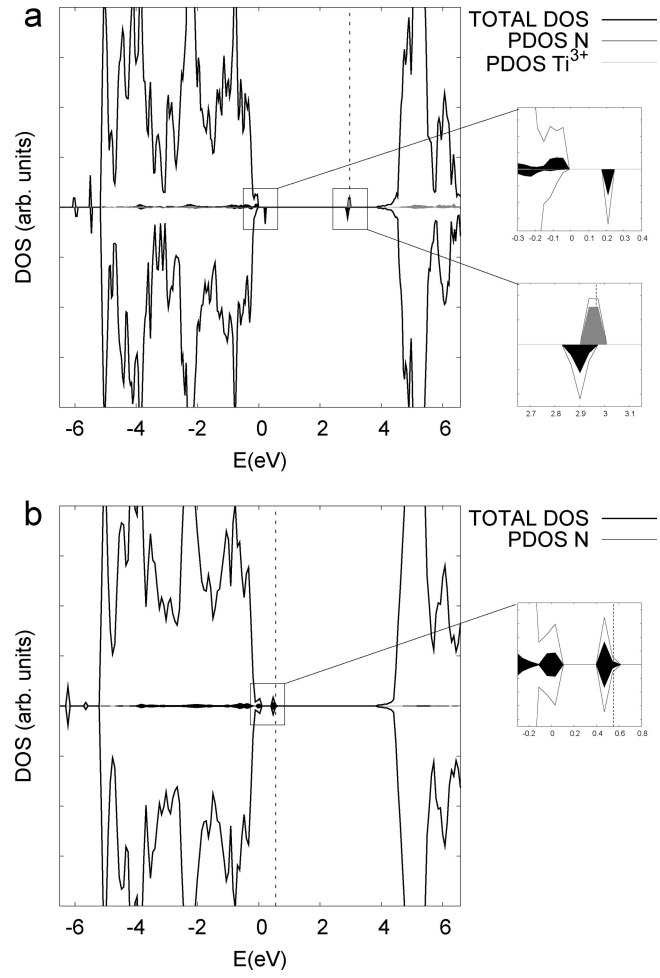

Figure 2. Total and projected (black, on N atom; grey, on Ti atom) density of states from the B3LYP calculation for the (a) triplet and (b) singlet N_s−F_s/TiO_2. The zero energy value is set at the top of the valence band. States below and above the dotted vertical line are occupied and unoccupied, respectively.

(26) Pacchioni, G.; Frigoli, F.; Ricci, D.; Weil, J. A. *Phys. Rev. B* **2001**, *63*, 054102.
(27) Mackrodt, W. C.; Simson, E.-A.; Harrison, N. M. *Surf. Sci.* **1997**, *384*, 192.
(28) Di Valentin, C.; Pacchioni, G.; Selloni, A. *Phys. Rev. Lett.* **2006**, *97*, 166803.
(29) Nambu, A.; Graciani, J.; Rodriguez, J. A.; Wu, Q.; Fujita, E. *J. Chem. Phys.* **2006**, *125*, 094706.
(30) Batzill, M.; Morales, E. H.; Diebold, U. *Phys. Rev. Lett.* **2006**, *96*, 026103.
(31) Nakano, Y.; Morikawa, T.; Ohwaki, T.; Taga, Y. *Appl. Phys. Lett.* **2005**, *86*, 132104.
(32) Sutter, E.; Sutter, P.; Fujita, E.; Muckerman, J. *Abstracts of the European Materials Research Society Spring Meeting*, Nice, France, 2006; European Materials Research Society: Strausbourg, France, 2006; p M-14.
(33) Weidmann, J.; Dittrich, Th.; Kostantinova, E.; Lauermann, I.; Uhlendorf, I.; Koch, F. *Sol. Energy Mater. Sol. Cells* **1999**, *56*, 153.
(34) Mills, A.; Lee, S.-K. *J. Photochem. Photobiol., A: Chem.* **2002**, *152*, 233.
(35) Kato, H.; Kudo, A. *J. Phys. Chem. B* **2002**, *106*, 5029.

Table 1. B3LYP Energy Differences in eV According to Scheme 2, Obtained from the Eigenvalues Computed at Γ Point with CRYSTAL06 Code

system	E_g	ΔE_{VB}	ΔE_{CB}
TiO_2	3.92		
N-doped TiO_2	3.90	0.11	
F-doped TiO_2	3.92		0.77
N−F/TiO_2−triplet	3.95	0.10	0.89
N−F/TiO_2−singlet	3.91	0.64	

gap of TiO_2 which is underestimated within the GGA.[36] Therefore, we have repeated the calculations of the triplet and singlet spin configurations for the N_s-F_s codoped system using the hybrid B3LYP functional (localized atomic basis set and CRYSTAL06 code). The main characteristics of the DOS and PDOS are not substantially different with respect to those obtained using the plane-wave GGA-PBE approach (Figure 2 vs Figure 1). The main differences are the band gap, which increases from 2.6 (PBE) to 3.9 eV (B3LYP),[12] and the position of the $3d^1$ Ti^{3+} defect state which is about 0.9 eV below the conduction band in the B3LYP calculation whereas it is at the conduction band edge with PBE. Details of the position of the impurity states in the band gap are reported in Table 1. Moreover, in the B3LYP calculation the gap state is fully localized on a single Ti^{3+} ion adjacent to the F impurity (see Figure 3). Given these differences, it is important to estimate the energy gain associated to the electron transfer from the Ti^{3+} $3d^1$ state to the N singly occupied 2p state, when going from the triplet ($N_s^{\bullet} + Ti^{3+}$) to the singlet configuration ($N_s^{-} + Ti^{4+}$). While the GGA-PBE provides a lower bound, B3LYP provides an upper bound (given the different estimates of the band gap). The stabilization energy, see $\Delta E_{T\text{-}S}$ in Scheme 2, amounts to 2.22 eV in B3LYP, to be compared with the previous value of 1.75 eV obtained with the PBE functional. On the basis of these data we confidently estimate that the actual value will be in this energy window.

A related important consequence of the internal electron transfer is the reduction in the energy cost to dope the material. By adding the energy costs of doping TiO_2 separately with N and with F and comparing the resulting value with the cost of codoping with the two species, one obtains a difference in energy of 1.8 (2.3) eV with PBE (B3LYP), according to the following equations:

$$TiO_2 + (1/2)N_2 \rightarrow TiO_{2-x}N_x + (1/2)O_2 \qquad \Delta E_r = 5.0\ (5.3)\ \text{eV} \quad (1)$$

$$TiO_2 + (1/2)F_2 \rightarrow TiO_{2-x}F_x + (1/2)O_2 \qquad \Delta E_r = -0.4\ (0.0)\ \text{eV} \quad (2)$$

$$TiO_2 + (1/2)N_2 + (1/2)F_2 \rightarrow TiO_{2-2x}N_xF_x + O_2 \qquad \Delta E_r = 2.8\ (3.0)\ \text{eV} \quad (3)$$

The codoping effect can thus be summarized in three main points which are all intimately interconnected: (i) charge compensation between a p-type (N) and an n-type (F) dopant through an internal charge transfer with a large stabilization effect; (ii) reduction of the number of oxygen vacancies associated with N-doping, resulting in less defective N−F/TiO_2 system; and (iii) reduction in the overall energy cost to dope the material.

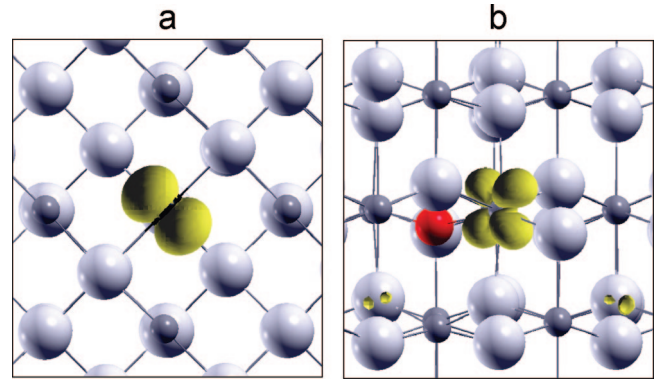

Figure 3. Spin density plots for the triplet spin configuration of N_s-F_s/TiO_2 as obtained with the B3LYP calculation: (a) localized spin on the N-atom and (b) localized spin on the Ti^{3+} cation adjacent to the F dopant.

Relevant structural parameters in anatase N−F/TiO_2 are reported in Figure 4a (PBE data) and Figure 4b (B3LYP data). In the triplet state the N−Ti and F−Ti bond lengths are similar to those observed for the separate N-doped and F-doped anatase TiO_2 systems.[11a,12] With the PBE functional, the bond lengths for Ti bound to the F dopant are typical of a Ti^{4+} center, as a consequence of the delocalization of the excess electron over a large number of Ti atoms. By contrast, with the B3LYP functional the excess electron is fully localized on a Ti atom that has an elongated Ti−O bond. This is a manifestation of the polaronic distortion which allows the charge trapping, as reported for other Ti^{3+} electron traps. Going from the triplet to the singlet configuration, with both functionals, the N−Ti bond lengths are strengthened and shortened as a result of the addition of a new bonding electron in the N 2p uppermost state. Since this is the consequence of the electron transfer and reoxidation of the Ti^{3+} to Ti^{4+}, the Ti−O bond lengths in the singlet state are those typical of a Ti^{4+} ion in both the PBE and B3LYP calculations.

4.1.2. N_i-F_s Codoping. It is generally believed that there are various possible configurations or chemical environments for nitrogen impurities in N-doped TiO_2, as suggested by the multiple features observed by XPS.[37,38] The relative abundance of the various N-containing species essentially depends on the method and conditions of the synthesis of the doped sample. In a previous work we have analyzed the possibility of having the N-dopant interstitially bound to a lattice O forming a N−O fragment tightly bound to the lattice Ti atoms (N_i).[11b] Here we consider the N-interstitial dopant, while leaving the F-atom in the substitutional site, since there is no evidence so far of other relevant locations for the F dopant in the lattice.[12,39–41] The DOS and PDOS for the

(36) Muscat, J.; Wander, A.; Harrison, N. M. *Chem. Phys. Lett.* **2001**, *342*, 397.
(37) Qiu, X.; Burda, C. *Chem. Phys.* **2007**, *339*, 1.
(38) Asahi, R.; Morikawa, T. *Chem. Phys.* **2007**, *339*, 57.
(39) Yu, J. C.; Yu, J.; Ho, W.; Jiang, Z.; Zhang, L. *Chem. Mater.* **2002**, *14*, 3808.
(40) Park, H.; Choi, W. *J. Phys. Chem. B* **2004**, *108*, 4086.
(41) Li, D.; Haneda, H.; Hishita, S.; Ohashi, N.; Labhsetwar, N. K. *J. Fluorine Chem.* **2005**, *126*, 69.

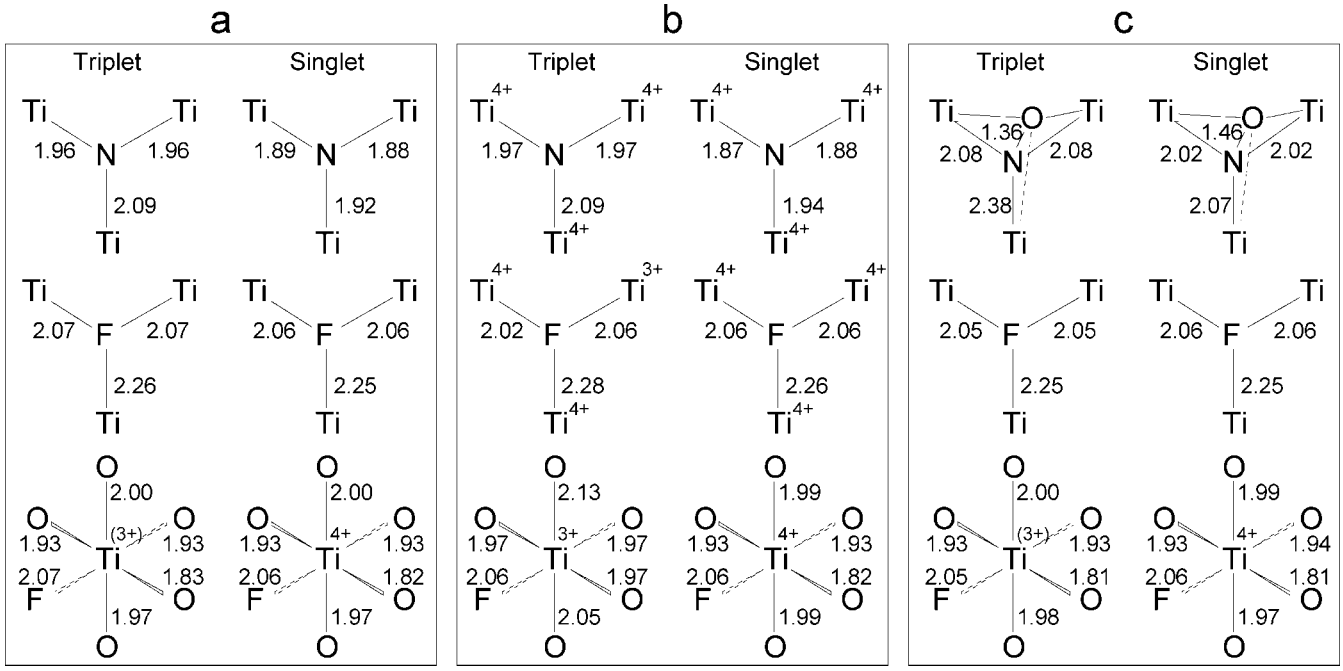

Figure 4. Details of the structural parameters (bond lengths) for some relevant bonds in N_s-F_s/TiO_2 (a, b) as obtained with the (a) PBE and (b) B3LYP functionals in the triplet and singlet spin configurations and in N_i-F_s/TiO_2 (c) as obtained with the PBE functional in the triplet and singlet spin configurations.

codoped N_i-F_s system are reported in Figure 5. These have been computed at the PBE level only: as discussed above for N_s-F_s codoping, except for the localization properties, the electronic structures calculated with the PBE and the B3LYP functionals are qualitatively similar. We first consider the triplet state ($N_i^{\bullet} + Ti^{3+}$, see Figure 5a). Also in this case the triplet electronic structure is the result of the superposition of the electronic structures of the two unperturbed separated N_i-doped and F_s-doped systems. In agreement with our previous calculations,[11b] the N-impurity states are found to lie higher in energy than for the substitutional case and are essentially π and π^* states of the N−O fragment. The DOS projected on the impurity atoms indicates the substantial localization of the dopant derived states. The projection on Ti atoms (not reported) shows the delocalized nature of the state hosting the excess electron associated to the F impurity, as already discussed for the N_s-F_s codoped triplet configuration. In the singlet state, the overall spin configuration of the system becomes a closed shell singlet ($N_i^{-} + Ti^{4+}$, see Figure 5b), as the unpaired electron of the Ti 3d state pairs with that in the highest π^* state of the N−O fragment. Similarly to what we found for the N_s-F_s codoped system, this electron transfer induces a large energy stabilization, ΔE, of 1.34 eV (Scheme 2), and also a structural deformation which confirms the occurrence of an electron transfer from Ti 3d to NO π^*: the N−O bond length increases from 1.36 to 1.46 Å (see Figure 4c).

In conclusion, the N_s-F_s/ and N_i-F_s/TiO_2 systems do not qualitatively differ in the essential features of the electronic structure. They differ for the details of the position of the impurity states and for the extent of stabilization energy resulting from the codoping effect.

4.2. Experimental Characterization of the Codoped Materials. The XRD patterns of N/TiO_2 (b) and $N-F/TiO_2$ (c, N/F = 1) materials are compared in Figure 6 with the reference spectrum of bare TiO_2, prepared with the same procedure. All samples show the XRD pattern typical of the anatase polymorph. The sharp peaks in the case of the $N-F/TiO_2$ (Figure 6c) indicate the occurrence of relatively larger crystallites than those obtained for the other two materials and possibly also a less defective sample.

The photocatalytic activity of the three sol−gel prepared materials have been compared by performing some preliminary tests, consisting in the degradation of an aqueous solution of methylene blue under monocromatic visible light ($\lambda = 437$ nm) irradiation. This is a standard, widely employed reaction for a rough evaluation of the photocatalytic potential of titania based powders. In Figure 7 the results of these tests are reported in terms of the amount of the decomposed dye as a function of time for the three different systems considered in the present work: TiO_2, N/TiO_2, and $N-F/TiO_2$. The data for the degradation of methylene blue in the absence of the catalyst is also enclosed for comparison (Figure 7a). The catalytic tests confirm what was already reported by Li and co-workers[9] indicating a clear increase of the catalytic activity for the N−F codoped material in comparison with that of all the other samples. The catalytic effect related to the presence of fluorine is however complex, and it will not be discussed further in this paper as it requires the detailed analysis of the role of F when incorporated in the bulk and when adsorbed at the surface.[39,42]

The DR UV−vis spectra of the prepared materials are reported in Figure 8. For the doped samples the typical absorption edge due to electronic transitions from valence

(42) (a) Minero, C.; Mariella, G.; Maurino, V.; Pelizzetti, E. *Langmuir* **2000**, *16*, 2632. (b) Minero, C.; Mariella, G.; Maurino, V.; Pelizzetti, D.; Vione, E. *Langmuir* **2000**, *16*, 8964.

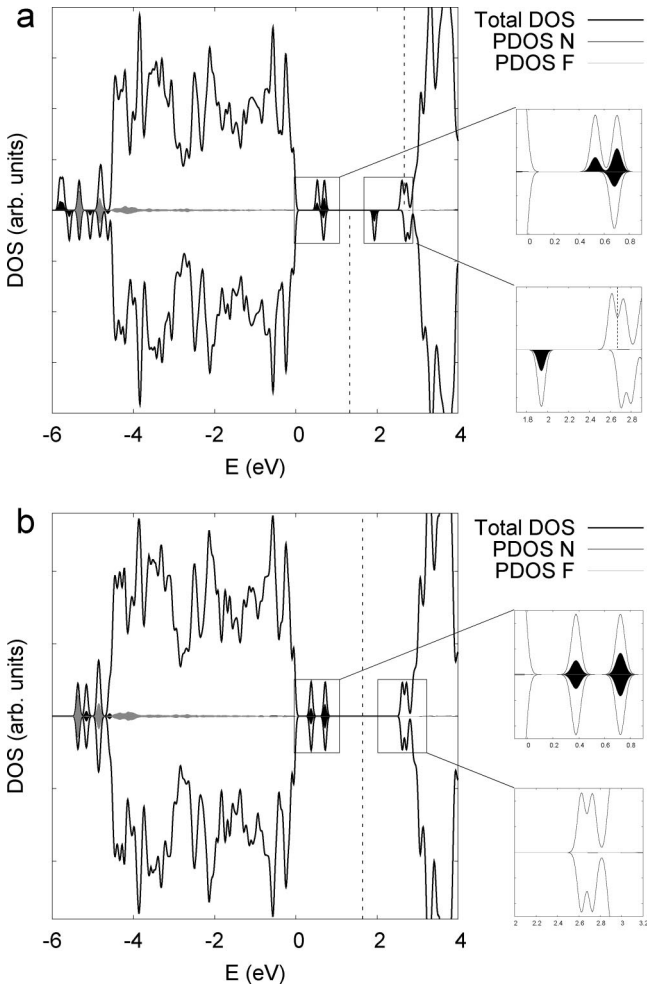

Figure 5. Total and projected (black, on N atom; grey, on F atom) density of states from the PBE calculation for the (a) triplet and (b) singlet N_i-F_s/TiO_2. The zero energy value is set at the top of the valence band. States below and above the dotted vertical line are occupied and unoccupied, respectively.

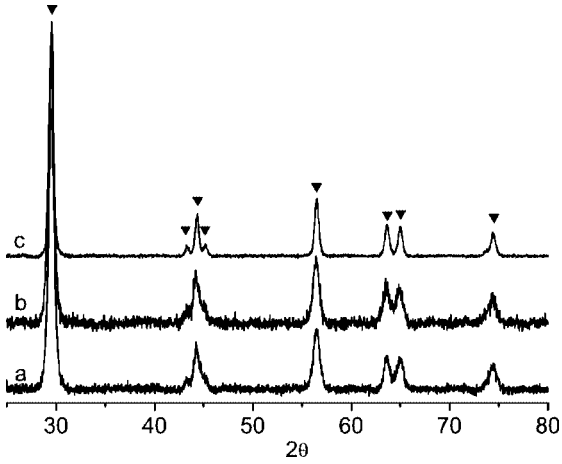

Figure 6. X-ray diffraction patterns of bare TiO_2 (a), N/TiO_2 (b), and $N-F/TiO_2$ (N/F = 1) (c) prepared by sol−gel synthesis and calcined at 770 K in air.

band to conduction band of TiO_2 (Figure 8a) is modified by the onset of a relatively broad absorption band in the visible region (Figure 8 b−e) whose intensity depends on the type of sample. This band is more intense for $N-F/TiO_2$ (N/F = 1) and progressively decreases in the following order: N/F = 10, N/F = 100, N-TiO_2. This absorption in the visible region is similar to those reported in the literature for N-doped titania and is associated to the impurity states deriving from nitrogen insertion in the bulk of the oxide.[9b,10] The concomitant presence of nitrogen and fluorine in the material definitely enlarges this optical feature in the spectrum. Its intensity is proportional to the F content, indicating a determinant role of F in the promotion of N insertion in TiO_2 lattice. This observation is consistent with the result reported above from the theoretical calculations of a reduction of the energy cost of doping when both N and F impurities are simultaneously introduced in the lattice. The absorption edge observed for the sample with N/F = 1 is slightly blue-shifted (3.22 eV) with respect to those recorded for TiO_2 and N/TiO_2 (3.15 and 3.12 eV, respectively). This effect is observed also in the case of F/TiO_2 and is related to the presence of fluorine in the solid.[12]

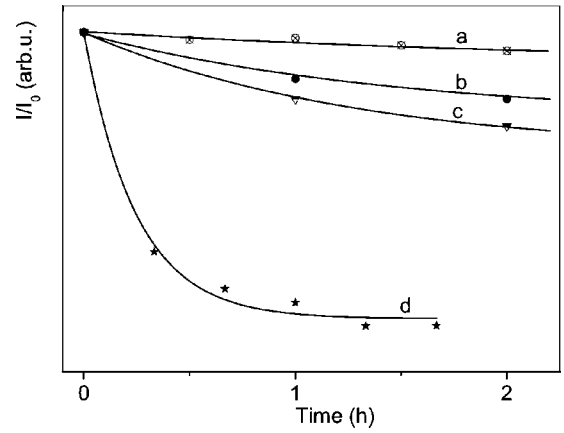

Figure 7. Photocatalytic activity in the methylene blue decomposition under visible light with λ = 437 nm of TiO_2 (b), N/TiO_2 (c), and $N-F/TiO_2$ (d, N/F = 1). Curve a: decomposition of the dye molecule in the absence of the catalyst.

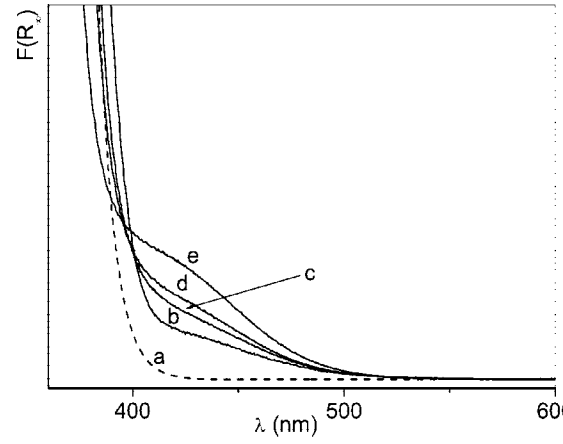

Figure 8. DR UV−vis spectra of bare TiO_2 (a), N/TiO_2 (b), and $N-F/TiO_2$ (c−e). N/F = 100, 10, and 1 for (c, d, and e, respectively).

The pivotal role of EPR spectroscopy in unraveling the nature of the defect states in the solid state is very well-known, and the potentiality of the technique in monitoring the extrinsic defects in titanium dioxide has already been exploited in the recent past.[11] The $N-F/TiO_2$ sample with N/F = 1 ratio exhibits, at 77 K, the spectrum reported in

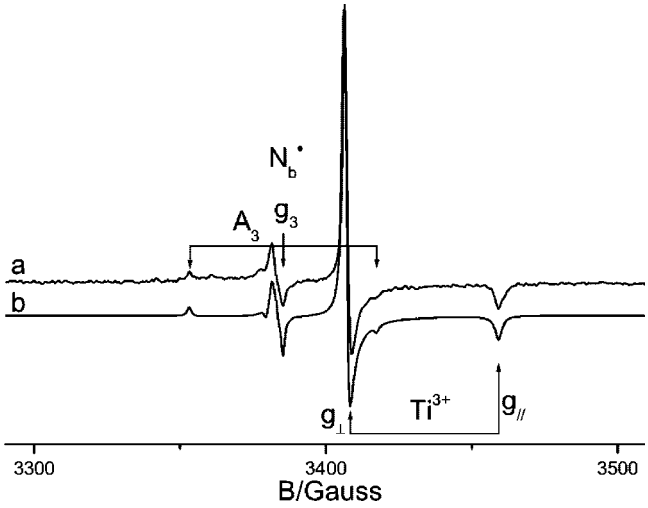

Figure 9. EPR spectrum and computer simulation of N−F/TiO_2 (N/F = 1). Spectrum recorded at 77 K.

Figure 9 with the corresponding computer simulation. The latter one suggests that the spectrum is the overlap of two distinct signals whose features are summarized in Table 2.

The first signal is due to the N containing species located in the bulk of the oxide already observed in previous work on N/TiO_2 and labeled $N_b^{\bullet}$. The spin Hamiltonian parameters of this species (which bears a hyperfine structure due to the interaction of the unpaired electron with the N nucleus) closely corresponds to those calculated for a nitrogen atom in the interstitial position in the TiO_2 lattice (N_i).[11b] In such conditions, as described above, the atom sticks to an oxygen ion of the lattice giving rise to a paramagnetic species with the unpaired electron in one of the π^* orbitals of the N−O fragment. The energy level of the species, as shown by the reported theoretical calculations and by EPR experiments under irradiation with visible light[11d] lies some tenths of an electronvolt over the valence band of TiO_2. An EPR signal with features and parameters not very different from those in Figure 9 is expected also in the case of the presence of substitutional nitrogen.

The second signal has no visible hyperfine structure and an axial **g** tensor with both parallel and perpendicular components lower than 2.0023 ($\mathbf{g}_e$) which can unambiguously be assigned to Ti^{3+} ions in the lattice. As in many cases of Ti^{3+} species the relaxation time T_2 is small enough to cause the broadening of the signal at $T > 77$ K so that at room temperature the same signal is barely observable. The presence of Ti^{3+} in the solid is a direct consequence of the inclusion of F in the structure.[12] The spin Hamiltonian parameters and the relative abundance of the two paramagnetic species, both derived by the computer simulation (Figure 9b), are reported in Table 2. This method, in the case of overlap of different signals, is much more accurate than a direct integration of the two signals. Interestingly the Ti^{3+} species is nearly 1 order of magnitude more abundant than the nitrogen one (0.88:0.12). A fraction of the nitrogen content in the solid is (as expected by the theoretical calculations shown above) in the diamagnetic negative form N_b^-. Though this species is EPR silent, its existence has been put into evidence, in the case of N/TiO_2, by experiments performed irradiating the solid with visible light ($\lambda = 437$ nm) and monitoring the increase of $N_b^{\bullet}$ due to the selective excitation of one of the two coupled electrons of the N_b^- HOMO orbital.[11d] Also in the present case (N−F/TiO_2) visible light irradiation causes an increase in the number of $N_b^{\bullet}$ centers.

From integration of the two peaks discussed above for a series of registered EPR spectra it is possible to provide a rough estimate of the concentration of the paramagnetic N_b and Ti^{3+} species present in lattice: 4×10^{13} spin/g and 3×10^{14} spin/g, respectively.

The calculations reported in the first part of the present paper point to the occurrence of an electron transfer between bulk defects (see Scheme 2) which can be summarized by the following equation:

$$Ti^{3+} + N_b^{\bullet} \leftrightarrow Ti^{4+} + N_b^- \quad (4)$$

If reaction 4 is not complete, that is, an equilibrium is established, all four species exist. This could explain why the spectrum in Figure 9 shows that both $N_b^{\bullet}$ and Ti^{3+} signals survive in the codoped material. Even if we assume that the process is complete and the equilibrium is totally shifted to the right, the presence of the paramagnetic species Ti^{3+} and $N_b^{\bullet}$ can have other origins. First, as already mentioned, the bulk concentration of the two dopants is not necessarily the same as they have different propensity to enter in the structure. Second, the sample is not completely homogeneous, presenting microcrystals with slightly different N/F relative content. Related to what was just considered, it is interesting to report the following analysis. In the case of a higher bulk concentration of fluorine (hence Ti^{3+}) than of nitrogen, one could expect that all $N_b^{\bullet}$ centers disappear owing to the electron transfer from excess Ti^{3+} species. On the contrary, if we examine both the results of (a) UV−vis absorption (Figure 8, see discussion above) and (b) the EPR intensity of $N_b^{\bullet}$ in the series of three samples with different

Table 2. Spin Hamiltonian Parameters and Relative Abundance of Observed Paramagnetic Species in N−F/TiO_2 Prepared with Different N/F Ratios

paramagnetic species	Ti^{3+}		$N_b^{\bullet}$					
EPR parameters	$g_{\|\|}$	$g_\perp$	g_1	g_2	g_3	A_1/G	A_2/G	A_3/G
	1.99	1.94	2.005	2.004	2.003	2.3	4.4	32.2
N/F in solution	relative abundance of the paramagnetic species							
1[a]	0.88		0.12					
10	0.75		0.25					
100			1.0					

[a] Spectrum in Figure 9.

nominal N/F ratios (Table 2, spectra available as Supporting Information, Figure S2) we conclude that (a) the amount of incorporated N increases with increasing F concentration in solution and is maximum for N/F = 1; (b) with an opposite trend, the fraction of $N_b^{\bullet}$ increases with decreasing F concentration and is maximum for N/F = 100. From the combined analysis of these results we can infer that the presence of fluorine actually increases the $N_b^{-}/N_b^{\bullet}$ ratio according to the process in eq 4.

Summarizing the experimental investigation has put into evidence the following facts: (a) both F and N can be incorporated in the structure of anatase; (b) the presence of fluorine favors nitrogen incorporation; (c) the presence of fluorine increases the catalytic activity of N−F/TiO_2 in comparison with that of N/TiO_2; (d) the presence of the two dopants generates shallow (Ti^{3+}) and deep (N_b^{-} − $N_b^{\bullet}$) localized states in the band gap; and (e) a partial electron transfer occurs between shallow and deep states (according to eq 4 and Scheme 2).

Conclusions

The codoping with nitrogen and fluorine gives rise to some remarkable effects as proven by the experimental results on the sol−gel prepared materials: (i) the incorporation of nitrogen is favored in the presence of fluorine, and (ii) the vis-light absorption and (iii) the photocatalytic activity under visible light irradiation are enhanced with respect to the singly doped materials. While in a first approximation one would assume that the codoped N−F/TiO_2 system behaves like the superposition of the two singly doped materials with the simultaneous presence of both shallow and deep localized states into the band gap, we have shown in this work that the situation is more complex. DFT calculations show a large stabilizing effect connected to the charge compensation between a p-type (N) and an n-type (F) dopant, through an internal charge transfer from the high lying Ti^{3+} 3d to the low lying N states. This process largely reduces the overall energy cost to dope the material (from about 5 to 3 eV) and occurs with no need to generate extra electrons by oxygen vacancy formation, opposite to what was reported in the case of N/TiO_2.[11b,d,29–31] This has the relevant consequence that a smaller number of oxygen defects are expected to be present in the bulk of the N−F codoped TiO_2 samples than in the N-doped counterpart and is probably the reason for the larger photostability and photocatalytic activity of the codoped sample.

Acknowledgment. This work has been supported by the Italian MIUR through a Cofin 2005 project and by the European COST action D41 "Inorganic oxide surfaces and interfaces". A.S. acknowledges support from the AFOSR MURI Grant F49620-03-1-0330.

Supporting Information Available: The spin density plot for the triplet spin configuration of N_s−F_s/TiO_2 as obtained with the PBE calculation and the N−F codoped TiO_2 EPR spectra recorded at RT are reported (PDF). This information is available free of charge via the Internet at http://pubs.acs.org.

CM703636S